Published September 7, 2017

Pedology

Measurement of Soil Color: A Comparison Between Smartphone Camera and the Munsell Color Charts

Zhaosheng Fan*
Jeffrey E. Herrick
USDA–ARS
Research Unit at the Jornada
2995 Knox St.
Las Cruces, NM 88003-8003

Rick Saltzman
SEEC, Suite N290
4001 Discovery Dr.
Boulder, CO 80303

Christina Matteis
Anna Yudina
Nicholas Nocella
Edward Crawford
Rick Parker
Dep. of Computer Science
Univ. of Colorado
1111 Engineering Dr.
Boulder, CO 80309

Justin Van Zee
USDA–ARS
Research Unit at the Jornada
2995 Knox St.
Las Cruces, NM 88003-8003

Soil color is one of the most useful soil properties for assessing and monitoring soil health. Here we present results of tests of a new soil color app for mobile phones. Various smartphone cameras (SPCs) were tested under sunny and cloudy conditions and compared with visual estimates using Munsell color charts (MCCs). The measured and estimated soil colors were then compared with the "true" colors determined using a spectrophotometer. The results indicated that soil color determinations based on SPC measurements under both sunny and cloudy conditions were as good as those obtained using the MCCs. The accuracy of the SPC measurements was affected by the natural illumination conditions, with higher accuracy in the sun than where clouds were present. Our results also indicated that the SPC measurements completed in the sun provide higher precision (lower variance) than SPC measurements completed under cloudy conditions or estimates based on MCCs. These results suggest that mobile-device cameras have great potential to allow non–soil scientists, and others lacking access to color charts, to determine soil color.

Abbreviations: CIE, International Commission on Illumination; MMC, Munsell color chart; sRGB, standard red-green-blue color space; SPC, smartphone camera.

Strong relationships have been established between soil color and many other important soil properties and characteristics, including mineral composition, soil fertility, soil organic matter content, soil moisture, soil drainage class, and land suitability (Baumann et al., 2016; Evans and Franzmeier, 1988; Franzmeier et al., 1983; Sanchez-Maranon et al., 2015; Schwertmann, 1993; Wills et al., 2007). Hence, soil color is an important indicator and attribute that can be used to characterize, classify, and differentiate soils (Aitkenhead et al., 2013).

The most common way to determine soil color is by comparison with Munsell color charts (MCCs) (Pendleton and Nickerson, 1951; Thompson et al., 2013). These charts define soil color based on three color dimensions: (i) hue, which indicates shade; (ii) value, which indicates lightness, and (iii) chroma, which indicates saturation (Pendleton and Nickerson, 1951; Viscarra Rossel et al., 2006). However, soil color observed using MCCs is strongly influenced by environmental conditions (e.g., illumination) and by the knowledge, experience, and color vision (e.g., normal versus deficient) of the observers. Therefore, soil color observed using MCCs is subjective and lacks consistency among different observers (Stiglitz et al., 2016a). Finally, it is challenging to generate reliable, quantitative, or statistical relationships between Munsell color and the corresponding soil properties due to the cylindrical coordinates (hue, value, and chroma) used by the Munsell color system (Ibanez-Asensio et al., 2013; Kirillova et al., 2015).

As a result, many recent studies have proposed alternative methods to more accurately and consistently measure soil color. One of the most promising alternative methods is to use mobile-phone cameras to measure soil color (Gomez-Robledo et al., 2013; Moonrungsee et al., 2015; Stiglitz et al., 2016b) or to use smartphone-

Core Ideas

- **Smartphone cameras can be used to reliably measure soil color.**
- **Soil color measured with smartphone cameras had less subjectivity and uncertainty.**
- **Natural lighting conditions affected the accuracy of the soil color measured with smartphone cameras.**

Soil Sci. Soc. Am. J. 81:1139–1146
doi:10.2136/sssaj2017.01.0009
Received 6 Jan. 2017.
Accepted 10 May 2017.
*Corresponding author (zhaosheng.fan@ars.usda.gov).

connected color sensors to conduct soil classification based on the soil color measured by those sensors (Aitkenhead et al., 2016; Han et al., 2016). However, most published studies that used smartphone cameras (SPCs) to measure soil color were limited to controlled illumination conditions (i.e., a controlled light source) in the laboratory (e.g., Gomez-Robledo et al., 2013) or required a separate sensor (e.g., Stiglitz et al., 2016b). The capability of SPCs to determine soil color has not been compared with Munsell-based determinations under natural, variable outdoor conditions where soil color is commonly determined.

The objective of this study was to investigate the accuracy and precision of a new smartphone camera app to measure soil color under natural outdoor lighting conditions and to compare the results with those based on ocular determinations with a Munsell Color Chart.

MATERIALS AND METHODS

The overall approach was to determine soil color using various SPCs and MCCs and then to compare the determined soil color with the "true" soil color measured using a spectrophotometer to investigate the performance of SPC measurements versus MCC-based estimates. We also compared soil color determined under two different natural illumination conditions—sunny (i.e., full sun) and cloudy (i.e., sun obscured by clouds)—to investigate how natural illumination conditions affect the accuracy and precision of the soil color measurements. In the following sections, we present the procedures of production, processing, and comparison of soil color in detail.

Sample Collection and Preparation

Thirty-three soils representing a broad range of soil colors and textures were used in this study. The soils were collected from the United States (Iowa, Nevada, New Mexico, and Utah) and Mexico (Aguascalientes, Chihuahua, Durango, Jalisco, and Zacatecas). After the soils were transported to the laboratory, they were air-dried and passed through a 2-mm sieve. A sample (~40 g) was removed from each of the 33 sieved soils with a mechanical soil splitter. Sand, silt, and clay contents were analyzed using a hydrometer (Gee and Or, 2002) or hand texturing (Thien, 1979) by an experienced soil scientist. Supplemental Table S1 lists the locations, Munsell color notations, and soil textures for the samples used in this study.

One of the objectives of this study was to examine the reliability of using SPCs to measure soil color under natural illumination conditions. Therefore, air-dried, disturbed soils were used in this study to minimize the impacts of nonsoil materials (e.g., roots) and soil moisture content on soil color. We hope that the findings with the disturbed soils can establish a foundation for further studies with undisturbed soils.

Digital Soil Color Acquisition with Smartphone Cameras

Eleven sets of three replicate photographs of each of the 33 soil samples were acquired. These photographs were acquired under both sunny and cloudy lighting conditions with a variety of mobile phone cameras in the spring of 2016 in Boulder, CO. Each photograph included the soil and a reference gray card (width, 12.7 cm; height, 7.6 cm) (CameraTrax) (Fig. 1). To test the technology across as broad a range of realistic outdoor conditions as possible with a limited budget, members of the development team were asked to acquire the images using their own cameras. Soil images that were taken with the cameras used under both sunny and cloudy conditions were compared to separate the effect of the device from lighting effects. All of the soil images have a resolution of 72 dots per inch and were taken between 12 and 2 pm with the camera flash off.

Fig. 1. Examples of the soil images with reference greycard taken when the sun was obscured by clouds (top panel) and under full sun (bottom panel).

Digital Soil Color Processing

The standard red-green-blue (sRGB) color space created by the smartphones is device dependent; that is, sRGB color space depends on the devices that create, capture, produce, and display the color. Therefore, the device-dependent sRGB color space was first transformed to device-independent color space, International Commission on Illumination (CIE) LAB or $L^*a^*b^*$ developed by the International Commission on Illumination, so the soil images produced by the different smartphones could be compared. More importantly, the CIE $L^*a^*b^*$

color space is much closer to and encompasses the entire range of human vision. For the CIE $L^*a^*b^*$ color space, the L^* value indicates lightness, where a higher L^* value indicates lighter color; the a^* value indicates color in red and green, where more positive a^* values indicate redder color and more negative values indicate greener color; and the b^* value indicates yellow and blue color, where more positive b^* values indicate yellower color and more negative values indicate bluer color. In the following paragraphs, we present the procedures of the transformation from sRGB to CIE LAB color space (Fig. 2).

For an image of a given soil sample, the nonshadow area of the soil image was first cropped to 200 × 200 pixels. The dominant sRGB values of the cropped soil image were then obtained using the modified median cut algorithm of color quantization (http://www.leptonica.com/color-quantization.html) (Bostock and Heer, 2009). Briefly, the soil image was reduced from 24-bit (16,777,216 colors) to 4-bit (16 colors) using the modified median cut quantization algorithm, and the color with highest population among the 16 colors was defined as the dominant color (R_s for the dominant red color value, G_s for the dominant green color value, and B_s for the dominant blue color values of the cropped soil image).

The nonshadow area of the image of the reference greycard, which was taken together with the soil image, was also cropped to 200 × 200 pixels. The dominant sRGB values of the cropped greycard image were obtained using the same modified median cut quantization algorithm (R_c for the dominant red color value, G_c for the dominant green color value, and B_c for the dominant blue color value of the cropped greycard image).

The "true" dominant sRGB values of the greycard were obtained using a spectrophotometer (CM-600d, Konica Minolta Sensing Inc.). This was a one-time measurement to obtain the "true" dominant sRGB values because we used the same greycard with all of the smartphones (R_{ct} for the "true" red color value, G_{ct} for the "true" green color value, and B_{ct} for the "true" blue color value of the reference greycard).

The dominant sRGB values of the soil images were then corrected based on the dominant sRGB values of the greycard by using the following equations:

$$R_{sa} = R_s \times R_{corr} \quad [1]$$

$$G_{sa} = G_s \times G_{corr} \quad [2]$$

$$B_{sa} = B_s \times B_{corr} \quad [3]$$

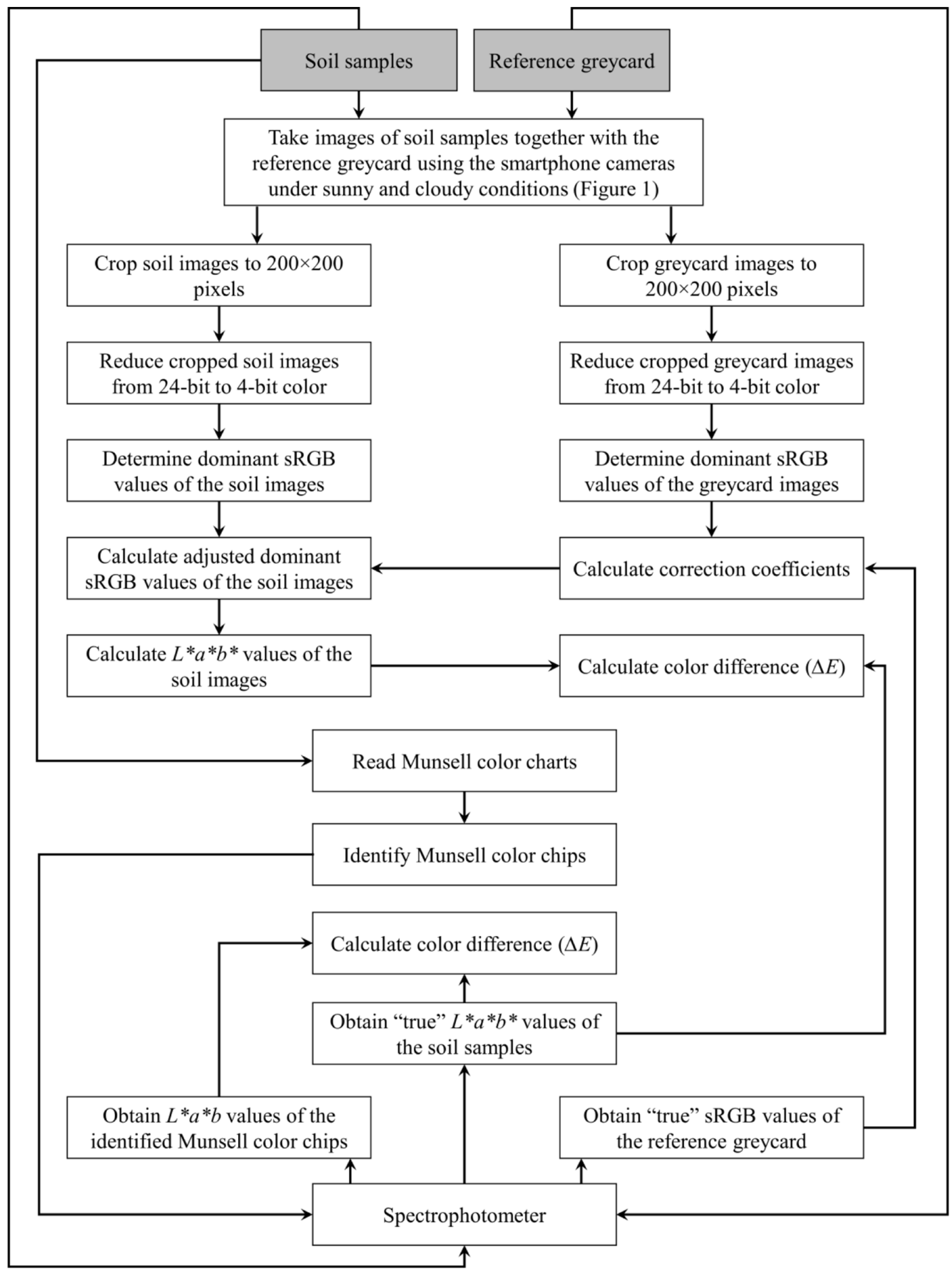

Fig. 2. Flowchart of the soil-image production and processing, transformation of soil images from standard red-green-blue color space (sRGB) to *L*a*b values in the CIELAB color space, and the subsequent calculations of the color differences between the *L*a*b** values measured using the smartphone cameras (SPCs) versus the "true" *L*a*b** values and between the *L*a*b** values measured with the Munsell color charts (MCCs) versus the "true" *L*a*b** values. The *L*a*b** values determined using the spectrophotometer were considered as the "true" values.**

Table 1. Smartphones used under sunny (full sun) and/or cloudy illumination conditions.

Illumination condition	Smartphone	Total number of images for each subsample†
Sunny only	HTC Wildfire and Samsung Admire	6
Cloudy only	iPhone 6	3
Sunny and cloudy	Motorola DROID Turbo,‡ HTC M8, and Samsung Galaxy S3	12

† For a given illumination condition and soil sample, a set of three replicate images was taken with each of the smartphone cameras.

‡ Motorola DROID Turbo was used to take soil images on two different days (one day is the day when the other smartphones were used, and the other day is when only the Motorola DROID Turbo was used).

where R_{sa}, G_{sa}, and B_{sa} are the corrected red, green, and blue color values of the soil images, respectively, and R_{corr}, G_{corr}, and B_{corr} are the linear correction coefficients for red, green, and blue color, respectively, and are defined as:

$$R_{corr} = R_{ct}/R_c \quad [4]$$

$$G_{corr} = G_{ct}/G_c \quad [5]$$

$$B_{corr} = B_{ct}/B_c \quad [6]$$

The corrected soil images were first transformed from sRGB to XYZ values (Tristimulus values; D_{65} illumination and 2° observer) in the CIE XYZ color space following Valous et al. (2009), and the XYZ values were then transformed to $L^*a^*b^*$ values in the CIE LAB color space following Robertson (1990).

Soil Color Comparison

After the sRGB values of soil images were transformed to $L^*a^*b^*$ values, the color difference (ΔE) between the $L^*a^*b^*$ values of a soil image and the "true" $L^*a^*b^*$ values of that soil sample were calculated. The "true" $L^*a^*b^*$ values were assumed to be the values measured using the spectrophotometer. The ΔE value between a soil image and the "true" value was calculated using the CIEDE2000 method following Sharma et al. (2005). A smaller ΔE value indicates a smaller difference between two colors.

Munsell Color Charts

We also matched each soil sample with the closest Munsell color chart (MCC) color chip and compared the color of the corresponding chip with the color of the soil generated by the SPC. For a given soil sample, this was completed as follows (Fig. 2). In Step 1, the MCC matching the color of the soil sample was identified between 12 and 2 pm in direct sunlight with the sun behind the observers. In Step 2, the $L^*a^*b^*$ values of the identified color chip were determined using the spectrophotometer. In Step 3, ΔE between the $L^*a^*b^*$ values of the identified color chip and the "true" $L^*a^*b^*$ values of that soil sample (i.e., L^*a^*b values measured using spectrophotometer) were calculated using the CIEDE2000 method.

The same five novice observers repeated Steps 1 to 3 for all 33 soil samples.

Statistical Analysis

We used a paired two-sample t test with a significance level (α) of 0.05 to determine if the measured color using different methods (e.g., ΔE for soil color determined with the SPCs under the sunny versus cloudy conditions or MCCs vs. SPCs) were significantly different. We also calculated the RMSE to compare L^*, a^*, and b^*values determined using the SPCs and MCCs with the standard values determined with the spectrophotometer:

$$\mathrm{RMSE}_L = \sqrt{\frac{\sum_{i=1}^{m}\left(L_{s,i} - L_i^{\#}\right)^2}{m}} \quad [7]$$

$$\mathrm{RMSE}_a = \sqrt{\frac{\sum_{i=1}^{m}\left(a_{s,i} - a_i^{\#}\right)^2}{m}} \quad [8]$$

$$\mathrm{RMSE}_b = \sqrt{\frac{\sum_{i=1}^{m}\left(b_{s,i} - b_i^{\#}\right)^2}{m}} \quad [9]$$

where RMSE_L, RMSE_a, and RMSE_b are the RMSE for L^*, a^*, and b^*values; m is the number of data points; $L_{s,i}$, $a_{s,i}$, and $b_{s,i}$ are the L^*, a^*, and b^*values for the ith soil sample determined using either the SPCs or the MCCs; and $L_i^{\#}$, $a_i^{\#}$, and $b_i^{\#}$ are the "true" L^*, b^*, and a^* values of the ith soil sample measured using the spectrophotometer.

RESULTS AND DISCUSSION

For each of the 33 soil samples, approximately 18 measurements were completed with the SPCs under sunny conditions (Table 1) and 15 under cloudy conditions (Table 1). A total of five estimates of each sample (one per observer) were completed using MCCs. The ΔE valueswere calculated between the $L^*a^*b^*$ values of each image (or each chip of MCCs) and the "true" $L^*a^*b^*$ values determined using the spectrophotometer. As a result, there were 594 measurements (18 per soil sample × 33 soil samples) with the SPCs under sunny conditions, 495 measurements (15 per soil sample × 33 soil samples) with the SPCs under cloudy conditions, and 155 estimates (5 per soil sample × 33 soil samples) with the MCCs.

The mean ΔE (± SD) of all soil measurements (i.e., the mean of the 594 ΔE_s) with the SPCs under sunny conditions (denoted as $\Delta \underline{E}_s$) was 6.45 ± 2.26. The mean ΔE of all measurements (i.e., the mean of the 495 ΔE_s) with the SPCs under cloudy conditions (denoted as $\Delta \underline{E}_c$) was 8.05 ± 3.46 SD. The mean ΔE of all estimates (i.e., the mean of the 155 ΔE_s) based on comparisons with the MCCs under sunny conditions (denoted as $\Delta \underline{E}_m$) was 7.41 ± 3.49. A ΔE value of 2.3 is generally understood to be the just-noticeable-difference threshold (Mokrzycki and Tatol, 2011), with a ΔE of 0.0 indicating that two colors are identical and a ΔE of 100.0 indicating that two colors are opposite (e.g., black and white). A study under

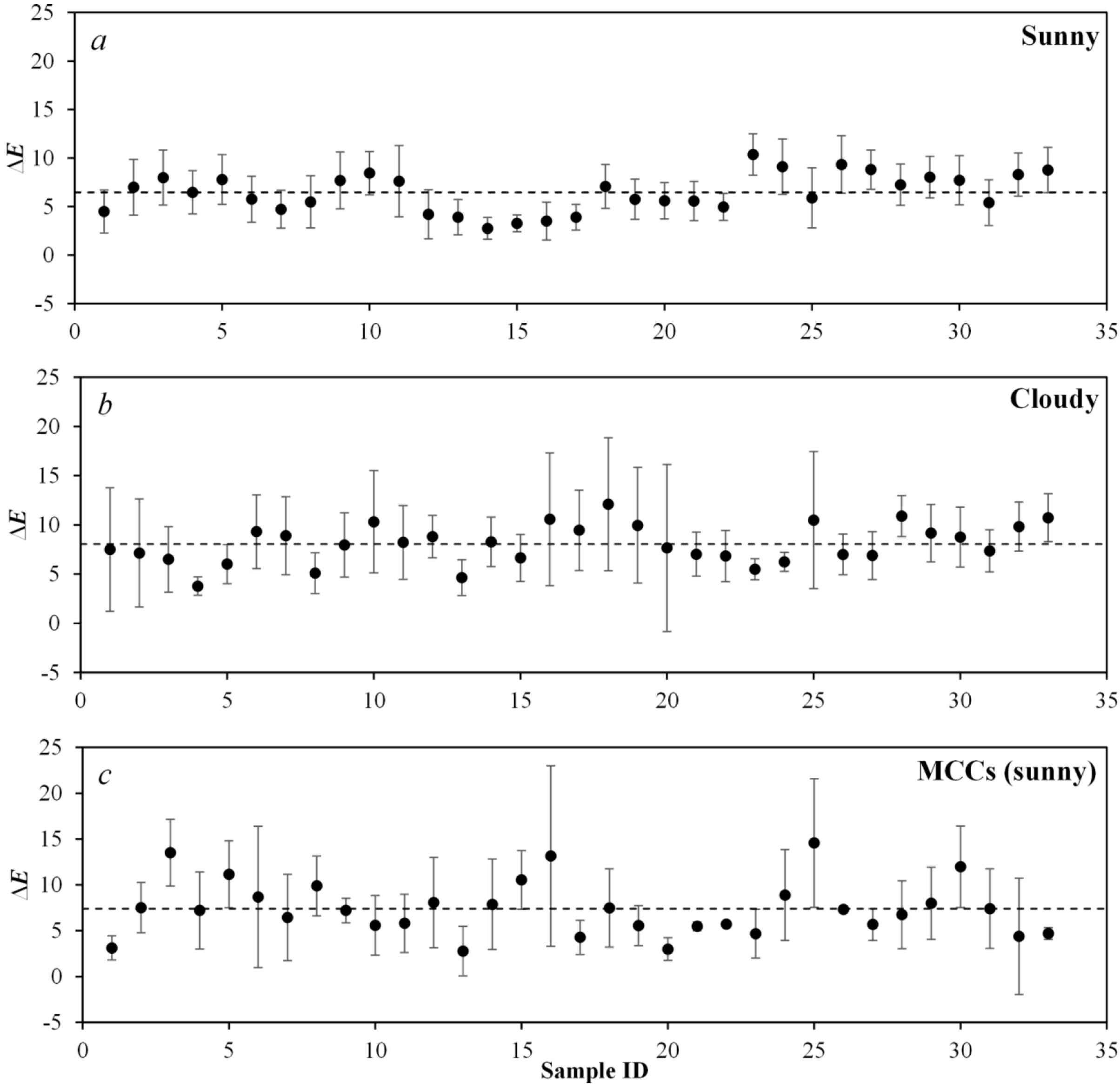

Fig. 3. The calculated color difference (*ΔE*) for each soil sample using smartphone cameras (SPCs) under sunny (full sun) and cloudy conditions and using the Munsell color charts (MCCs). For the SPCs under sunny (a) and cloudy (b) conditions, each data point represents the mean *ΔE* of all images (i.e., 18 and 15 images, respectively; Table 1) taken for the corresponding soil sample. For the MCC determinations (c), each data point represents the mean *ΔE* of the images from five independent human observations from the spectrophotometer-determined value for each soil sample. Error bars represent SDs from the mean (*n* = 18 for under sunny conditions, *n* = 15 for under cloudy conditions, and *n* = 5 for MCCs). The dashed line represents the mean *ΔE* of all images taken with the SPCs (under sunny or cloudy conditions) or MCCs.

indoor, controlled conditions showed that the threshold for the human eye to distinguish color differences in chromatically manipulated images of landscapes ranged from 1.2 to 4.0 (Aldaba et al., 2006).

For a given soil sample, we also calculated the mean ΔE for all measurements of each soil sample; therefore, the mean ΔE for a given soil sample was calculated as the mean of the 18 ΔE_s with the SPCs under sunny conditions (denoted as $\Delta \underline{E}_s$), the mean of the 15 ΔE_s with the SPCs under cloudy conditions (denoted as $\Delta \underline{E}_c$), and the mean of the five ΔEs with the MCCs (denoted as $\Delta \underline{E}_m$). The paired *t* test among $\Delta \underline{E}_s$, $\Delta \underline{E}_c$, and $\Delta \underline{E}_m$ (Fig. 3; Table 2) indicated that there was no significant difference between $\Delta \underline{E}_s$ and $\Delta \underline{E}_m$ ($p = 0.14$) or between $\Delta \underline{E}_c$ and $\Delta \underline{E}_m$ ($p = 0.30$). These results indicated that soil color measured by the SPCs under both sunny and cloudy conditions was similar to that observed by human vision with the MCCs, suggesting that using SPCs to measure soil color under natural illumination in the field is as reliable as using MCCs, at least for relatively novice observers.

Table 2. The *p* values based on the paired Student's *t* test between the mean of the 18 color difference values with the smartphone cameras under sunny conditions (denoted as $\Delta \underline{E}_s$), the mean of the 15 color difference values with the smartphone cameras under cloudy conditions (denoted as $\Delta \underline{E}_c$), and the mean of the five color difference values with the Munsell color chart (denoted as $\Delta \underline{E}_m$).

	$\Delta \underline{E}_s$	$\Delta \underline{E}_c$	$\Delta \underline{E}_m$
ΔE_s	–	0.003	0.14
ΔE_c	0.003	–	0.30
ΔE_m	0.14	0.30	–

Table 3. The calculated root mean square errors of *L, *a**, and *b** values for the soil images taken using the smartphone cameras under sunny (full sun) and cloudy conditions and using the Munsell color charts (MCCs).**

Illumination condition	Smartphone	RMSE†		
		L^* ($RMSE_L$)	a^* ($RMSE_a$)	b^* ($RMSE_b$)
Sunny	Droid Turbo	6.21	2.86	2.04
	HTC M8	3.13	1.84	1.64
	HTC Wildfire	5.70	1.89	2.71
	iPhone 6	–	–	–
	Samsung Admire	9.27	2.61	5.46
	Samsung Galaxy S3	7.97	3.60	3.00
	Overall	6.92	2.70	3.49
Cloudy	Droid Turbo	8.02	3.41	4.43
	HTC M8	7.20	6.08	7.03
	HTC Wildfire	–	–	–
	iPhone 6	7.06	1.84	4.67
	Samsung Admire	–	–	–
	Samsung Galaxy S3	10.43	3.41	3.95
	Overall	9.40	3.59	4.67
MCCs		7.67	2.26	3.80

† Calculated using Eq. [7–9]

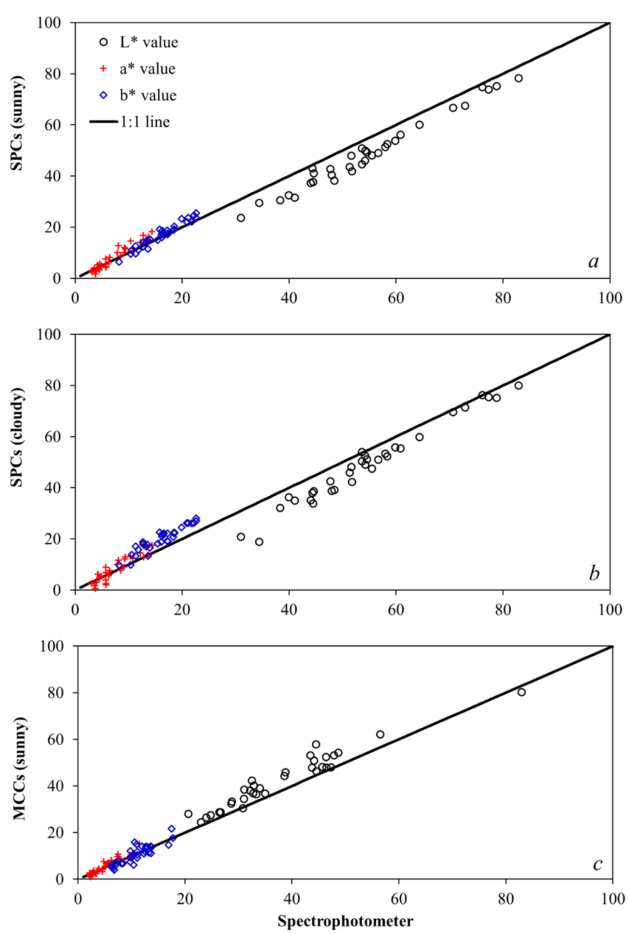

Fig. 4. Comparison of *L, *a**, and *b** values measured using the spectrophotometer versus those measured using smartphone cameras (SPCs) under sunny conditions (full sun) (a), SPCs under cloudy conditions (b), and Munsell color charts (MCCs) under sunny conditions (c). For the MCCs, each of the data points represents the mean value of five independent observations for each of the soil samples. For the SPCs, each of the data points represents the mean value of all images (i.e., 18 and 15 images under the sunny and cloudy conditions, respectively; Table 1) taken for the corresponding soil sample.**

The paired *t* test among $\Delta\underline{E}_s$, $\Delta\underline{E}_c$, and $\Delta\underline{E}_m$ (Fig. 3; Table 2) indicated that there was a significant difference between $\Delta\underline{E}_s$ and $\Delta\underline{E}_c$ (p = 0.003). As presented above, $\Delta\underline{E}_s$ (6.45) is smaller than $\Delta\underline{E}_c$ (8.05). Also, soil color measured under sunny conditions tended to have a smaller RMSE than that measured under cloudy conditions (Table 3). Although some of the phones used under sunny and cloudy conditions were not same, the calculated RMSEs for Droid Turbo, HTC M8, and Samsung Galaxy S3 (the three phones used under both sunny and cloudy conditions) were also lower under sunny conditions than under cloudy conditions (Table 3). These findings suggest that natural illumination conditions (sunny versus cloudy) affected the accuracy of the measured soil color and that the accuracy of soil color was higher under sunny than cloudy conditions, although both sunny and cloudy SPC soil colors were similar to the color determined using the MCCs under sunny conditions.

The mean SDs were overall smaller for $\Delta\underline{E}_s$ than for $\Delta\underline{E}_c$ and $\Delta\underline{E}_m$ (2.26, 3.46, and 3.49 for $\Delta\underline{E}_s$, $\Delta\underline{E}_c$, and $\Delta\underline{E}_m$, respectively) (Fig. 3). The 95% confidence intervals of the mean SDs were smaller for $\Delta\underline{E}_s$ than for $\Delta\underline{E}_c$ and $\Delta\underline{E}_m$ (0.20, 0.69, and 0.77 for the mean SDs of $\Delta\underline{E}_s$, $\Delta\underline{E}_c$, and $\Delta\underline{E}_m$, respectively) (Fig. 3). Taken together, these results indicate that the uncertainty of soil color measured with the SPCs under sunny conditions was smaller than the uncertainty of the soil color measured with the SPCs under cloudy conditions and with the MCCs, suggesting that bright ambient light (e.g., direct sunlight) could reduce the uncertainty associated with the identified soil color using SPCs compared with low and more variable ambient light (e.g., cloudy conditions).

Changes in L^* values correspond to changes in "value" of the Munsell color space. The L^* values measured using the MCCs were on average higher (Fig. 4; Table 4), translating to an approximately 0.5 Munsell value unit overestimation relative to that measured by the spectrophotometer. This suggests that soil color observed using the MCCs tended to be lighter (higher L^*) than the "true" soil color, which might be due to observer error. By comparison, the L^* values measured using the SPCs under sunny and cloudy conditions were on average lower by approximately the same magnitude (Fig. 4; Table 4). This suggests that the soil color measured using the SPCs under sunny and cloudy conditions tended to be darker (lower L^*) than the "true" soil color.

In comparison to L^* value, changes in a^* and b^* values correspond to changes in hue and chroma values of the Munsell color space. The a^* and b^* values measured with the SPCs under sunny

Table 4. Mean "true" *L, *a**, and *b** values and the mean measured *L**, *a**, and *b** values using the smartphone cameras (SPCs) and Munsell color charts (MCCs).**

CIE LAB color space	"True" value†	SPCs		MCCs
		Sunny	Cloudy	
L^*	54.7	48.8‡	49.3‡	61.3‡
a^*	7.3	8.3‡	8.0	7.9‡
b^*	15.9	16.9‡	20.0‡	15.5

† Measured using the spectrophotometer.

‡ The mean measured L^*, a^*, or b^* value was significantly different (i.e., $p < 0.05$) from the corresponding "true" value based on the paired t test on the mean L^*, a^*, and b^* values for each of the soil samples (Fig. 4).

Table 5. The coefficients of correlation between soil texture and deviations in the predicted CIE LAB values.

Soil texture	Deviation† in the predicted CIE LAB value		
	*L**	*a**	*b**
	SPCs (sunny)		
Sand, %	–0.44‡	–0.00	–0.16
Silt, %	0.50‡	0.11	0.13
Clay, %	0.18	0.16	0.13
	SPCs (cloudy)		
Sand, %	0.29	0.06	0.12
Silt, %	–0.26	–0.24	–0.23
Clay, %	–0.23	0.22	0.09

† The deviation is defined as the CIE LAB value measured with the smartphone cameras (SPCs) under sunny or cloudy conditions minuses the CIE LAB value measured with the spectrophotometer (Fig. 4).

‡ Significant at the 0.05 level.

conditions were on average higher (Fig. 4; Table 4). These results suggest that soil color measured with the SPCs under both sunny and cloudy conditions tended to be more yellow (higher *b**) and more red (higher *a**).

Further analyses indicated that there were no significant correlations between soil texture and the deviations in the measured CIE LAB values (i.e., *L**, *a**, and *b** values), except that the deviations in the measured *L** value with SPCs under sunny conditions were significantly correlated with sand % and silt % (Table 5). However, there were more and stronger significant correlations between soil color and the deviations in the measured CIE LAB values with SPCs (Table 6). These results suggest that the deviations between the measured soil color with SPCs and the "true" soil color measured with the spectrophotometer were more likely caused by soil color than by soil texture.

Although our studies showed that it is promising to use SPCs to measure soil color under outdoor natural illumination conditions, there may be considerable uncertainties (with the measured soil color) caused by many factors that are not included in our experiments but that may play important roles in the determination of soil color. First, air-dried soil samples were used in our studies; however, soil moisture content can affect soil color through directly altering soil albedo and visible/near infrared spectral reflectance (Post et al., 2000) and/or by altering soil redox conditions (O'Donnell et al., 2011) that further affect soil color due to the change in soil mineral composition (Vaughan et al., 2016). Second, the irregular shapes and arrangement of soil particles and aggregates can strongly affect soil surface roughness and thus the reflected incoming radiation from the surface of soil samples (Cierniewski et al., 2013; Matthias et al., 1998; Potter et al., 1987), which may result in different color determinations for two identical soils where one has been homogenized. Additional studies are needed to investigate how to minimize the uncertainty of measured soil color associated with soil heterogeneity while maintaining and capturing important variability within the soil (e.g., redoximorphic features). It is also possible that building an automated image resampling system into the app could help to address some of the variability issues. In this study, the soil images were cropped to 200 × 200 pixels (the first step of processing soil images).

Table 6. The coefficients of correlation between soil color and the deviations in the predicted CIE LAB values.

Soil color‡	Deviation† in the predict CIE LAB value		
	*L**	*a**	*b**
	SPCs (sunny)		
*L**	0.42§	–0.60§	0.01
*a**	–0.47§	0.69§	0.43§
*b**	–0.15	0.40§	0.58§
	SPCs (cloudy)		
*L**	0.65§	–0.59§	–0.06
*a**	–0.25	0.57§	0.29
*b**	–0.08	0.21	0.33

† The deviation is defined as the CIE LAB value measured with the smartphone cameras (SPCs) under sunny or cloudy conditions minuses the CIE LAB value measured with the spectrophotometer (Fig. 4).

‡ Soil color was measured using the spectrophotometer.

§ Significant at the 0.05 level.

CONCLUSIONS

The number of smartphone users was approximately 1.86 billion worldwide in 2015 and is predicted to be approximately 2.9 billion by 2020 worldwide (Statista, 2014). Therefore, there is a great potential for citizens without soils training to upload observations (e.g., soil color) with geospatial locations from mobile devices to soil databases (Rossiter et al., 2015; Silvertown, 2009) to dramatically and dynamically expand the current soil color database. More meaningfully, soil color measured with smartphone cameras might also be used by citizens and/or professionals to predict other important soil properties (e.g., soil organic matter content and soil fertility) (e.g., Wills et al., 2007) that may be used to estimate soil productivity. Therefore, further studies are needed to explore and establish the relationships between soil color and other soil properties (e.g., soil organic matter content). Nonetheless, our results suggest that smartphones and other mobile devices have the potential to significantly enhance our ability to quickly and reliably measure soil color in the field, making it possible for anyone with a cell phone and a reference card to facilitate the expanded use of soil color as an environmental indicator to support a wide variety of agricultural and environmental inventory, monitoring, assessment, and management.

ACKNOWLEDGMENTS

This research was based on work supported by the United States Agency for International Development, the USDA–ARS, and the Department of Computer Science at the University of Colorado. The authors thank Jason C. Neff and the Sustainability Innovation Lab at Colorado at the University of Colorado, Boulder, for providing logistical support and coordination of this study and two anonymous reviewers and the associate editor for their helpful comments. The use of trade, product, industry, or firm names is for descriptive purposes only and does not imply endorsement by the US government.

REFERENCES

Aitkenhead, M.J., M. Coull, W. Towers, G. Hudson, and H.I.J. Black. 2013. Prediction of soil characteristics and colour using data from the National Soils Inventory of Scotland. Geoderma 200-201:99–107. doi:10.1016/j.geoderma.2013.02.013

Aitkenhead, M.J., D. Donnelly, M. Coull, and R. Gwatkin. 2016. Estimating soil properties with a mobile phone. In: A.E. Hartemink and B. Minasny, editors, Digital soil morphometrics. Springer, Basel, Switzerland. p. 89–110.

doi:10.1007/978-3-319-28295-4_7

Aldaba, M.A., J.M.M. Linhares, P.D. Pinto, and S.M.C. Nascimento. 2006. Visual sensitivity to color errors in image of natural scenes. Vis. Neurosci. 23:555–559. doi:10.1017/S0952523806233467

Baumann, K., I. Schoning, M. Schrumpf, R.H. Ellerbrock, and P. Leinweber. 2016. Rapid assessment of soil organic matter: Soil color analysis and Fourier transform infrared spectroscopy. Geoderma 278:49–57 [erratum: 310:80]. doi:10.1016/j.geoderma.2016.05.012

Bostock, M., and J. Heer. 2009. Protovis: A graphical toolkit for visualization. IEEE Trans. Vis. Comput. Graph. 15:1121–1128. doi:10.1109/TVCG.2009.174

Cierniewski, J., A. Karnieli, K. Kusnierek, A. Goldberg, and I. Herrmann. 2013. Approximating the average daily surface albedo with respect to soil roughness and latitude. Int. J. Remote Sens. 34:3416–3424.

Evans, C.V., and D.P. Franzmeier. 1988. Color index values to represent wetness and aeration in some Indiana soils. Geoderma 41:353–368. doi:10.1016/0016-7061(88)90070-5

Franzmeier, D.P., J.E. Yahner, G.C. Steinhardt, and H.R. Sinclair. 1983. Color patterns and water table levels in some Indiana soils. Soil Sci. Soc. Am. J. 47:1196–1202. doi:10.2136/sssaj1983.03615995004700060027x

Gee, G.W., and D. Or. 2002. Particle-size analysis. In: J.H. Dane and G.C. Topp, editors, Methods of soil analysis. Part 4. Physical methods. SSSA, Madison, WI. p. 255–293.

Gomez-Robledo, L., N. Lopez-Ruiz, M. Melgosa, A.J. Palma, L.F. Capitan-Vallvey, and M. Sanchez-Maranon. 2013. Using the mobile phone as Munsell soil-colour sensor: An experiment under controlled illumination conditions. Comput. Electron. Agric. 99:200–208. doi:10.1016/j.compag.2013.10.002

Han, P., D. Dong, X. Zhao, L. Jiao, and Y. Lang. 2016. A smartphone-based soil color sensor: For soil type classification. Comput. Electron. Agric. 123:232–241. doi:10.1016/j.compag.2016.02.024

Ibanez-Asensio, S., A. Marquez-Mateu, H. Moreno-Ramon, and S. Balasch. 2013. Statistical relationships between soil colour and soil attributes in semiarid areas. Biosys. Eng. 116:120–129. doi:10.1016/j.biosystemseng.2013.07.013

Kirillova, N.P., Y.N. Vodyanitskii, and T.M. Sileva. 2015. Conversion of soil color parameters from the Munsell system to the CIE-L*a*b* system. Eurasian Soil Sci. 48:468–475. doi:10.1134/S1064229315050026

Matthias, A.D., A. Fimbres, E.E. Sano, D.F. Post, L. Accioly, A.K. Batchily, et al. 1998. Surface roughness effects on soil albedo. Soil Sci. Soc. Am. J. 64:1035–1041. doi:10.2136/sssaj2000.6431035x

Mokrzycki, W., and M. Tatol. 2011. Color difference Delta E: A survey. Machine Graphics Vision 20:383–411.

Moonrungsee, N., S. Pencharee, and J. Jakmunee. 2015. Colorimetric analyzer based on mobile phone camera for determination of available phosphorus in soil. Talanta 136:204–209. doi:10.1016/j.talanta.2015.01.024

O'Donnell, T.K., K.W. Goyne, R.J. Miles, C. Baffaut, S.H. Anderson, and K.A. Sudduth. 2011. Determination of representative elementary areas for soil redoximorphic features identified by digital image processing. Geoderma 161:138–146. doi:10.1016/j.geoderma.2010.12.011

Pendleton, R.L., and D. Nickerson. 1951. Soil colors and special soil color charts. Soil Sci. 71:35–44. doi:10.1097/00010694-195101000-00004

Post, D.F., A. Fimbres, A.D. Matthias, E.E. Sano, L. Accioly, A.K. Batchily, et al. 2000. Predicting soil albedo from soil color and spectral reflectance data. Soil Sci. Soc. Am. J. 64:1027–1034. doi:10.2136/sssaj2000.6431027x

Potter, K.N., R. Horton, and R.M. Cruse. 1987. Soil surface roughness effects on radiation reflectance and soil heat flux. Soil Sci. Soc. Am. J. 51:855–860. doi:10.2136/sssaj1987.03615995005100040003x

Robertson, A.R. 1990. Historical development of CIE recommended color difference equations. Color Res. Appl. 15:167–170. doi:10.1002/col.5080150308

Rossiter, D.G., J. Liu, S. Carlisle, and A.-X. Zhu. 2015. Can citizen science assist digital soil mapping? Geoderma 259-260:71–80. doi:10.1016/j.geoderma.2015.05.006

Sanchez-Maranon, M., A. Romero-Freire, and F.J. Martin-Peinado. 2015. Soil-color changes by sulfuricization induced from a pyritic surface sediment. Catena 135:173–183. doi:10.1016/j.catena.2015.07.023

Schwertmann, U. 1993. Relations between iron oxides, soil color, and soil formation. In: J.M. Bigham and E.J. Ciolkosz, editors, Soil color. SSSA, Madison, WI. p. 51–69.

Sharma, G., W. Wu, and E.N. Dalal. 2005. The CIEDE2000 color-difference formula: Implementation notes, supplementary test data, and mathematical observations. Color Res. Appl. 30:21–30. doi:10.1002/col.20070

Silvertown, J. 2009. A new dawn for citizen science. Trends Ecol. Evol. 24:467–471. doi:10.1016/j.tree.2009.03.017

Statista. 2014. Number of smartphone users worldwide from 2014 to 2020. Statistica, New York. https://www.statista.com/statistics/330695/number-of-smartphone-users-worldwide/ (accessed 3 Jan. 2017).

Stiglitz, R.Y., E.A. Mikhailova, C.J. Post, M.A. Schlautman, and J.L. Sharp. 2016a. Teaching soil color determination using an inexpensive color sensor. Natural Sciences Education 45. doi:10.4195/nse2016.03.0005

Stiglitz, R.Y., E.A. Mikhailova, C.J. Post, M.A. Schlautman, and J.L. Sharp. 2016b. Evaluation of an inexpensive sensor to measure soil color. Comput. Electron. Agric. 121:141–148. doi:10.1016/j.compag.2015.11.014

Thien, S.J. 1979. A flow diagram for teaching texture by feel analysis. J. Agron. Educ. 8:54–55.

Thompson, J.A., A.R. Pollio, and P.J. Turk. 2013. Comparison of Munsell soil color charts and the GLOBE soil color book. Soil Sci. Soc. Am. J. 77:2089–2093. doi:10.2136/sssaj2013.03.0117n

Valous, N.A., F. Mendoza, D.W. Sun, and P. Allen. 2009. Colour calibration of a laboratory computer vision system for quality evaluation of pre-sliced hams. Meat Sci. 81:132–141. doi:10.1016/j.meatsci.2008.07.009

Vaughan, K.L., F. Miller, N. Navarro, and C. Appel. 2016. Visual assessment of sulfate reduction to identify hydric soils. Soil Sci. Soc. Am. J. 80:1114–1119. doi:10.2136/sssaj2016.02.0035

Viscarra Rossel, R.A., B. Minasny, P. Roudier, and A.B. McBratney. 2006. Colour space models for soil science. Geoderma 133:320–337. doi:10.1016/j.geoderma.2005.07.017

Wills, S.A., C.L. Burras, and J.A. Sandor. 2007. Prediction of soil organic carbon content using field and laboratory measurements of soil color. Soil Sci. Soc. Am. J. 71:380–388. doi:10.2136/sssaj2005.0384